JOURNAL OF VIROLOGY, Apr. 2009, p. 3696–3703 Vol. 83, No. 8
0022-538X/09/$08.00+0 doi:10.1128/JVI.02464-08

Fewer Latent Herpes Simplex Virus Type 1 and Cytotoxic T Cells Occur in the Ophthalmic Division than in the Maxillary and Mandibular Divisions of the Human Trigeminal Ganglion and Nerve▽

Katharina Hüfner,[1] Anja Horn,[2] Tobias Derfuss,[1] Christine Glon,[1] Inga Sinicina,[3] Viktor Arbusow,[1] Michael Strupp,[1] Thomas Brandt,[4] and Diethilde Theil[1,4]*

Department of Neurology, Klinikum Grosshadern, Ludwig-Maximilians University, Munich, Germany[1]; Institute of Anatomy, Ludwig-Maximilians University, Munich, Germany[2]; Institute for Legal Medicine, Ludwig-Maximilians University, Munich, Germany[3]; and Department of Clinical Neurosciences, Klinikum Grosshadern, Ludwig-Maximilians University, Munich, Germany[4]

Received 1 December 2008/Accepted 2 February 2009

Following primary infection of the mouth, herpes simplex virus type 1 (HSV-1) travels retrogradely along the maxillary (V2) or mandibular (V3) nerve to the trigeminal ganglion (TG), where it establishes lifelong latency. Symptomatic HSV-1 reactivations frequently manifest as herpes labialis, while ocular HSV-1 disease is rare. We investigated whether these clinical observations are mirrored by the distribution of latent HSV-1 as well as cytotoxic T-cell infiltration around the nerve cell bodies and in the nerve fibers. The three divisions of the TG were separated by using neurofilament staining and carbocyanine dye Di-I tracing and then screened by in situ hybridization for the presence of HSV-1 latency-associated transcript (LAT). The T-cell distribution and the pattern of cytolytic molecule expression were evaluated by immunohistochemistry. The Di-I-labeled neurons were largely confined to the nerve entry zone of the traced nerve branches. Very few Di-I-labeled neurons were found in adjacent divisions due to traversing fiber bundles. LAT was abundant in the V2 and V3 divisions of all TG but was scarce or totally absent in the ophthalmic (V1) division. $CD8^+$ T cells were found in all three divisions of the TG and in the respective nerves, clearly clustering in V2 and V3, which is indicative of a chronic inflammation. Only T cells surrounding neurons in the V2 and V3 ganglionic divisions expressed granzyme B. In conclusion, the large accumulation of LAT and cytotoxic T cells in the V2 and V3 but not in the V1 division of the TG reflects the sites supplied by the sensory fibers and the clinical reactivation patterns.

Herpes simplex virus type 1 (HSV-1) is a double-stranded DNA virus that usually infects the vast majority of the human population before and during adolescence. Primary HSV-1 infection is in general either asymptomatic or manifests as stomatitis aphtosa. Following the primary infection, which commonly occurs via the mucous membranes of the mouth, the virus travels retrogradely along the maxillary (V2) or mandibular (V3) division of the trigeminal nerve. It then reaches the somata of the trigeminal ganglion (TG) cells, where it establishes lifelong latency. During latency, HSV-1 viral activity is restricted; only the latency-associated transcript (LAT) is abundantly expressed (28). LAT is engaged in establishing latency (31) and in facilitating the process of reactivation (6). At the same time, it promotes neural survival after HSV-1 infection by reducing apoptosis (19).

Symptomatic HSV-1 reactivations frequently manifest as herpes labialis (16) but only rarely as HSV-1 ocular disease (13). The cornea is the most frequent site of ocular herpetic disease, and inflammation of the cornea caused by HSV-1, "herpes stromal keratitis" (HSK), is the major infectious cause of blindness in the Western world (9). Once an episode of keratitis has occurred, recurrences are seen in 10% of patients/year (8, 13, 26). In humans, it is still a matter of debate whether a primary HSV-1 ocular infection has to occur in order for the virus to establish latency in the ophthalmic division (V1) of the TG. Findings from the HSV-1 animal model have shown that after HSV-1 lip inoculation, the virus can become latent in several ocular structures, probably through neural connectivity (12, 32). On the other hand, it has been demonstrated that HSV-1 can establish latency in the human cornea itself in patients suffering from HSK (9). This is supported by evidence from the HSV-1 mouse model, showing that HSK can reoccur without anterograde transport of the virus from the TG to the cornea (20).

In view of the latest findings from the HSV-1 mouse model (10) and humans (11, 29, 35) indicating that $CD8^+$ T cells accompanying HSV-1 latency are involved in maintaining HSV-1 in a latent state, we investigated the distribution of latent HSV-1, cytotoxic T cells, and granzyme B expression in the ophthalmic division versus maxillary and mandibular divisions of human TG. The respective nerves were traced to identify the somatotopic organization of the TG in order to accurately locate the occurrence of LAT, T cells, and granzyme B.

MATERIALS AND METHODS

Samples. The use of autopsy samples for the present study was approved by the Ethics Committee of the Medical Faculty of the Ludwig-Maximilians Uni-

* Corresponding author. Mailing address: Department of Neurology, Klinikum Grosshadern, Marchioninistr. 23, 81377 Munich, Germany. Phone: 49-89-7095-4816. Fax: 49-89-7095-4801. E-mail: diethilde.theil@med.uni-muenchen.de.

▽ Published ahead of print on 11 February 2009.

versity of Munich. Eighteen TG were removed 9 to 25 h after death (mean, 18.1 h) from 11 subjects (three females), whose ages ranged from 18 to 84 years (mean, 50.5 years). The cause of death was mainly related to trauma. For tracing, ganglia were handled as described in detail below; for immunohistochemistry and in situ staining, ganglia were embedded directly in Tissue Tek compound (Sakura, Zoeterwoude, The Netherlands). Frozen sections 8 to 15 μm thick were made and mounted on positively charged slides (SuperFrost/Plus; Menzel, Braunschweig, Germany). To evaluate the cytoarchitecture of the TG, sections were stained with 0.5% cresyl violet, revealing the somata of neural and glial cells, or were processed for fiber staining according to the silver impregnation protocol of Gallays (4).

Postmortem tracing with Di-I. To identify the trigeminal neural somata of the ophthalmic branch 13 TG were used for postmortem tracing with the carbocyanine dye Di-I using the "delayed-fixation" approach by Sparks (27). Of these, nine TG were used for anatomical analysis and four for the analysis of viral and immunological parameters. The TG was cleared of the meninges, and the ophthalmic branch was shortened to approximately 5 mm to minimize the tracing distance. Then the nerve stump was placed into a small plastic tube filled with a solution of 5 mg Fast Di-I (D-7756; Molecular Probes, Eugene, OR) dissolved in 30 μl dimethylformamide. The other trigeminal nerve branches were shielded with parafilm. The TG with the Di-I-filled tube was then covered with wet gauze and placed in a petri dish containing artificial cerebrospinal fluid (ACSF; 120 mM NaCl, 3 mM KCl, 1 mM $CaCl_2$, 1 mM $MgSO_4$, 26 mM $NaHCO_3$, 1.4 mM NaH_2PO_4, 10 mM D-glucose) at 4°C. After 10 to 14 days, ACSF was replaced by 4% paraformaldehyde (PFA) and the TG was stored for another 7 to 8 days at 4°C. It was then equilibrated in increasing concentrations of sucrose (10%, 20%, and 30%) in 0.1 M phosphate buffer for freeze cutting. As controls, the maxillary or mandibular branch of three TG was infiltrated with Di-I. The mounted sections were examined with a Leica DMRB microscope (Leica, Bensheim, Germany), and the distribution of Di-I-labeled neurons was plotted using Neurolucida software (MicroBrightField, Williston, VT). Photographs were taken with a digital camera (Pixera Pro 600 ES; Klughammer, Markt Indersdorf, Germany) using Viewfinder software (Klughammer) and were processed with Photoshop 7.0 software (Adobe, San Jose, CA). The sharpness, contrast, and brightness were adjusted to reflect the appearance seen through the microscope.

Immunohistochemistry. Immunohistochemical stainings were done with primary antibodies against T-cell markers (1:1,000 rabbit anti-human CD3 and 1:100 mouse anti-human CD8; Dako, Hamburg, Germany) and against neurofilament (1:500 rabbit anti-human neurofilament AB1982; Chemicon-Millipore, Hampshire, United Kingdom), and granzyme B (1:100 mouse anti-human granzyme B; Serotec, Düsseldorf, Germany) using a previously described protocol (29). In brief, frozen tissue sections were thawed, dried, fixed (acetone for granzyme B stainings, 4% PFA for all other stainings), and then sequentially incubated with 0.5 to 3% hydrogen peroxide for 10 min, 5% normal rabbit serum (when monoclonal antibodies were used), or 5% normal goat serum (when polyclonal antibodies were used) for 30 min. The diluted primary antibodies were left to incubate for 2 h at room temperature or overnight at 4°C. Afterwards, tissue sections were incubated for 30 min in biotinylated rabbit anti-mouse immunoglobulin G antibody (1:300; Dako) or biotinylated goat anti-rabbit immunoglobulin G antibody (1:300; Dako). The sections were incubated with peroxidase-conjugated streptavidin or AB complex (Dako) for 30 min and then incubated with diaminobenzidine (Dako) for up to 10 min. For the granzyme B staining, the protocol was modified so that the peroxidase-antiperoxidase (PAP) complex system (Dako) was used for detection. To assess CD3 and CD8 expression, the average total number of positive cells in three fields of view (magnification of ×400) was evaluated.

Immunostainings for nonphosphorylated neurofilament H were done as described below following a blocking reaction in 1% H_2O_2 in 0.1 M Tris-buffered saline (TBS) and an incubation in 5% normal horse serum with 0.3% Triton X-100 in TBS for 1 h. Sections were treated with mouse anti-nonphosphorylated neurofilament H (1:5,000 SMI-32; Sternberger Monoclonal Antibodies Incorporated, Baltimore, MD) for 48 h at 4°C. Sections were then incubated in horse anti-mouse serum (1:200; Vector Lab, Southfield, MI) in 0.1 M TBS containing 2% bovine serum albumin for 1 h at room temperature and then, after washing, in streptavidin peroxidase (1:1,000; Sigma, Deisenhofen, Germany) for 1 h. The antigenic site was visualized with diaminobenzidine.

LAT in situ and hybridization and FISH. The in situ protocol used was described in detail in a previous work (30). The LAT oligonucleotide probe was synthesized and labeled with digoxigenin (MWG-Biotech AG, Ebersberg, Germany). Tissue sections from each ganglion were hybridized with antisense LAT probes and then detected using alkaline phosphate-conjugated antidigoxigenin antibodies included in the DIG nucleic acid detection kit (Roche Molecular Biochemicals, Mannheim, Germany) and 5-bromo-4-chloro-3-indolyl phosphate–nitroblue tetrazolium (Roche Molecular Biochemicals). When fluorescent in situ hybridization (FISH) was applied, the LAT probes were detected with fluorescein-labeled antidigoxigenin antibodies (1:5; Roche Diagnostics, Mannheim, Germany). For quantification, all LAT-positive neurons in the respective division of the TG, as identified by Di-I labeling or neurofilament staining, were counted. Again, several separate sections of each TG were evaluated in parallel.

RESULTS

Histology of the TG. The overall distribution of neural cell bodies within the TG is clearly demonstrated in sections stained for nonphosphorylated neurofilament H (NP-NF), which is present only in neurons but not in glial cells, as seen in cresyl violet-stained sections (Fig. 1 A). Its convex face gives rise to the three main branches (V1, V2, and V3) of the trigeminal nerve. The analysis of serial sections through the TG revealed that the cell bodies form a more or less continuous crescent-shaped group with only poor segregation of the subdivision, which is most pronounced between the ophthalmic and maxillary subdivisions (Fig. 1A). Silver staining shows that the corresponding fiber bundles extend beyond the cell bodies, thereby defining the three TG regions more clearly, before they merge to form the compact sensory root of the trigeminal nerve proximally (Fig. 1B). After optimal tissue fixation in 4% PFA, all trigeminal neurons including their emerging axons express strong immunostaining for NP-NF immediately upon removal (Fig. 1C). After Di-I labeling, the NP-NF immunostaining was weaker; however, many TG neurons were still strongly stained for NP-NF and they did not show major signs of disintegration (Fig. 1D).

Tracing of the TG with Di-I. After a total tracing interval of 17 to 22 days following Di-I application to the ophthalmic trigeminal branch, the nerve fibers showed a strong red fluorescence (Fig. 2A and C), and labeled cells were detected around the entry zone of the ophthalmic nerve (Fig. 2A and C). The Di-I-labeled cells exhibited an intensive diffuse red fluorescence that filled the whole cell body (Fig. 2D), whereas an autofluorescence signal visible with all fluorescence filters was confined to lipofuscin granules in tracer-negative neurons (Fig. 2E). The systematic analysis of traced TG revealed that the Di-I-labeled neurons were largely confined to the portion of the TG around the entry zone of the traced ophthalmic or maxillary nerve (Fig. 2A and B). Only a very small number of Di-I-labeled neurons were also found in the adjacent divisions of the TG, as defined by the traversing fiber bundles of the TG nerve branches, which was not due to tracer contamination of the neighboring nerve branches (Fig. 2A and B).

LAT-positive neurons in the three divisions of TG. All of the 12 tested ganglia showed a positive hybridization signal for LAT. The absolute number of LAT-positive neurons was assessed on several separate single sections of each ganglion for the neurons projecting to each of the TG branches. The neurons projecting to the V2 and V3 branches of human TG contained significantly more LAT-positive neurons (V2, 13.7 ± 9.7; V3, 17.6 ± 10.5) than those of the V1 branch (0.8 ± 1.4; Kruskal-Wallis analysis of variance [ANOVA]; $P < 0.0001$; Fig. 3A and Fig. 4A to I). The number of LAT-positive neurons in the neurons projecting to the V2 and V3 branches was 10 to 20 times larger than those projecting to the V1 branch.

Distribution of CD3/CD8$^+$ T cells in the three divisions and nerves of the TG. CD3/CD8$^+$ T cells clustered around the

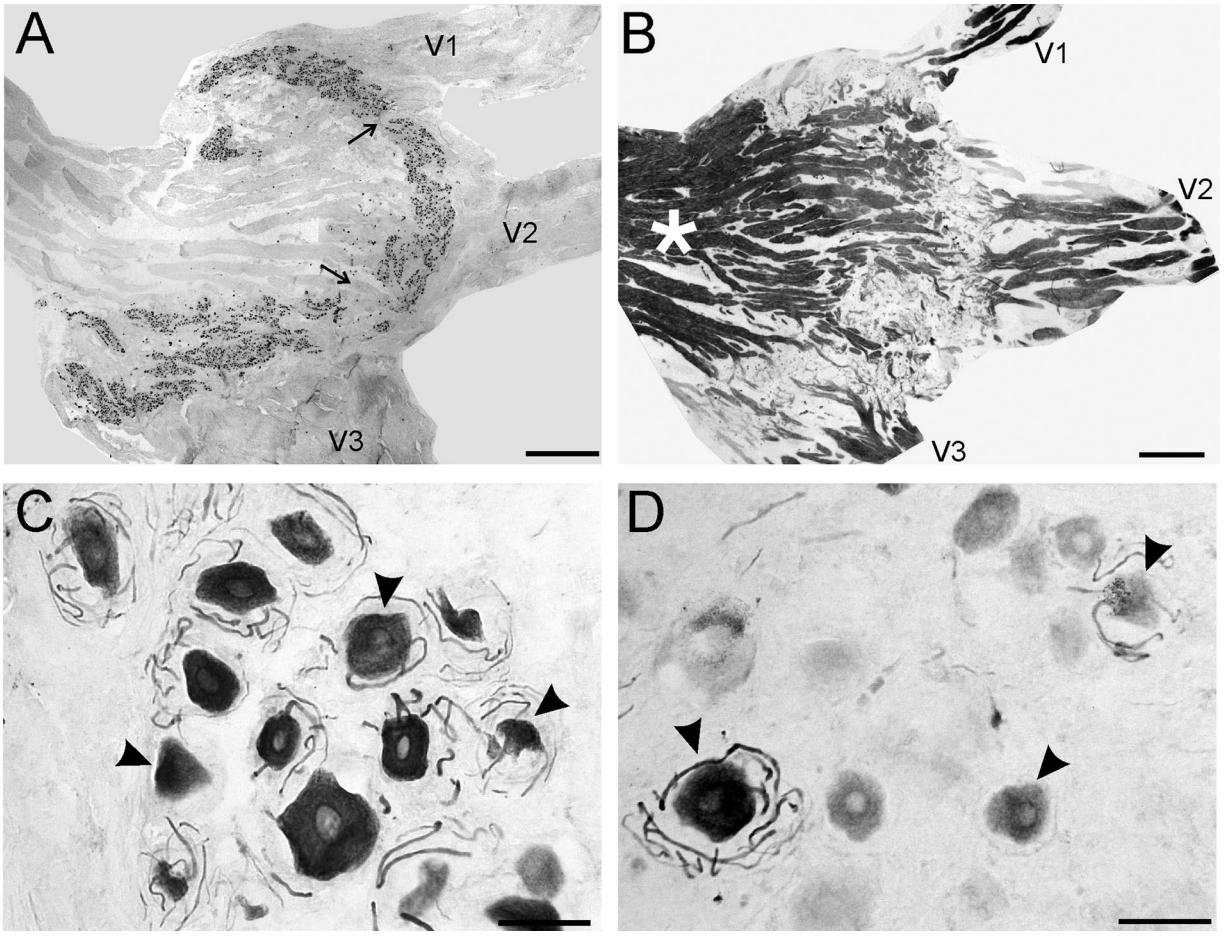

FIG. 1. Anatomy of the human TG. (A) Immunostaining for NP-NF demonstrates the distribution of neural cell bodies, and (B) silver impregnation (Gallyas) shows the course of nerve fibers in the TG. A clear-cut separation of all three divisions is not obvious (arrows in panel A), but can be expected, considering the nerve fiber course of the respective nerve branches. (B) Silver staining reveals that the corresponding fiber bundles form the compact sensory root of the trigeminal nerve proximally (asterisk). (C) High-power photograph of TG neurons stained for NP-NF of a TG processed for optimal histological preservation showing the morphology of the pseudounipolar ganglia cells and their axons (arrowheads). (D) TG neurons stained for NP-NF after exposure to Di-I using the "delayed-fixation approach." Note that fewer TG neurons are immunostained (arrowheads), but no major signs of disintegration of TG cells were seen. Scale bars: panels A and B, 2 mm; panels C and D, 50 μm.

neurons in the V2 and V3 portions of the TG (V2, 29.1 ± 11.2/field of view; V3, 33.7 ± 14.3/field of view), while significantly fewer T cells surrounded the neurons in the V1 branch (14 ± 8.1; Kruskal-Wallis ANOVA; $P = 0.0007$; Fig. 3B and 5A and C). T cells in the V1 branch were mostly single and scattered, not clustered. A significant correlation between the presence of CD3/CD8$^+$ T cells in the neurons projecting to the three branches of the TG and the presence of LAT was found (Spearman rank order correlations, 0.59; $P = 0.0001$). The T cells in the V2 and V3 branches of the TG expressed granzyme B as a marker of specific activation. Clusters of granzyme B-positive T cells were found in the V2 and V3 portions of the TG, while the V1 portion did not contain any clusters of granzyme B-positive T cells (Fig. 5E and F).

CD3$^+$ and CD8$^+$ T cells were also found in between the nerve fibers of the three nerve divisions. They were mainly clustered in the maxillary and mandibular nerves, and only a few T cells were scattered along the ophthalmic branch (Fig. 5B and D). The pattern of distribution of the T cells in the nerve branches closely resembled that seen in the ganglia.

DISCUSSION

This study investigated the occurrence of LAT and cytotoxic T cells in the three divisions of human TG and nerve.

To accurately separate the three divisions, TG were Di-l traced. Labeled neural bodies from the ophthalmic branch were predominantly found in the ophthalmic subdivision of the TG, and Di-I tracing from the maxillary or mandibular branch resulted in labeled neurons in the maxillary or mandibular subdivision of the TG. A very small number of additionally Di-I-labeled neurons were found in the transitional zone. Our observations on the location of Di-I-labeled neurons in the TG are in line with findings from tract tracer experiments in monkeys. Tracer injection into orbital structures, such as the cornea (17), extraocular muscles (21), eyelids (33), conjunctiva (23),

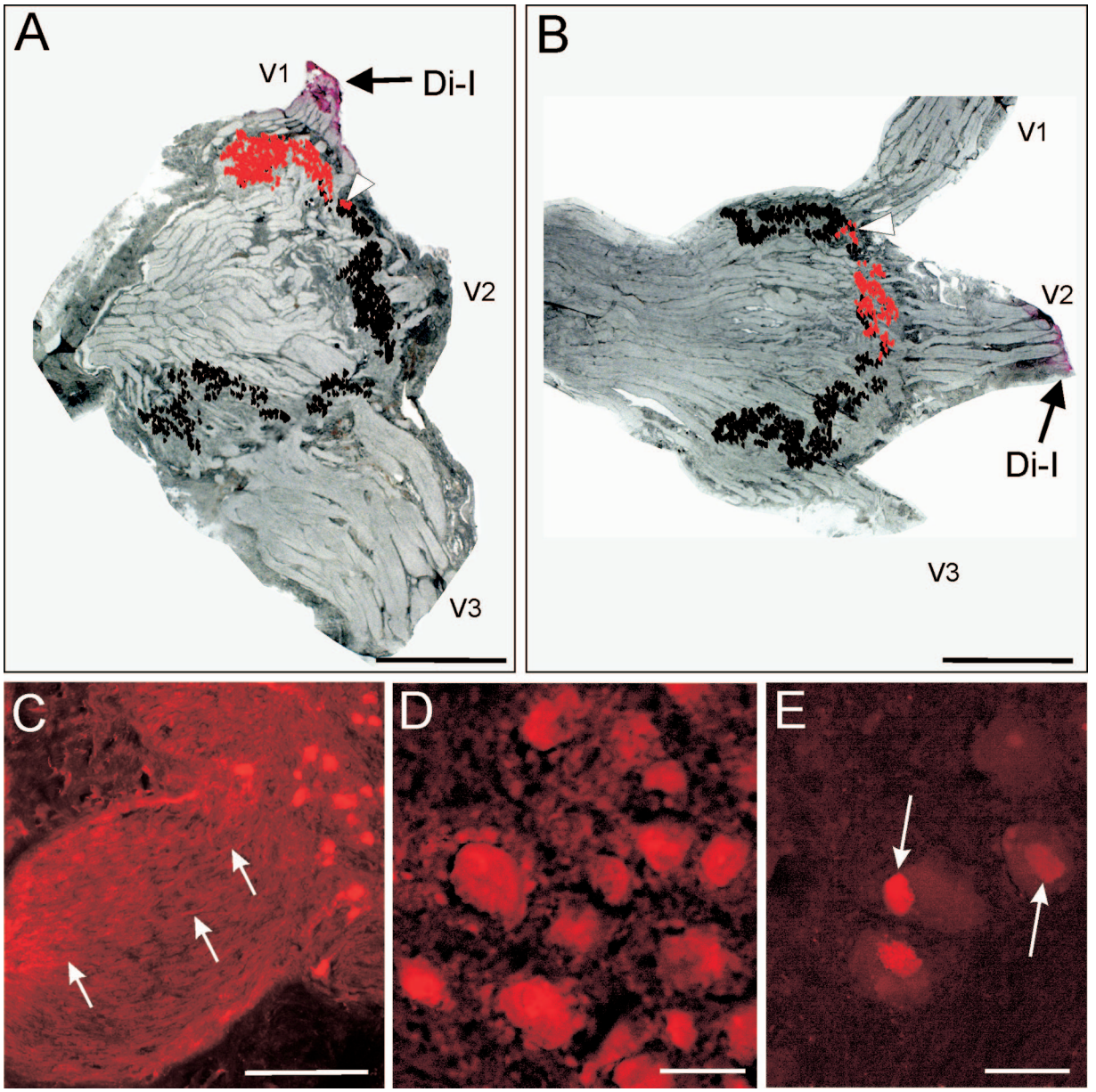

FIG. 2. Di-I tracing of the maxillary and mandibular branches of the human TG. Human TG showing the distribution of Di-I-labeled neurons (red dots) in comparison to unlabeled neurons (gray dots) after Di-I exposure to the ophthalmic (A) or the maxillary (B) branch. Only a very small number of Di-I-labeled neurons could also be found in the adjacent divisions of the TG as defined by the traversing fiber bundles of the TG nerve branches. This was not due to tracer contamination of the neighboring nerve branches (A and B, arrowheads). (C) Photograph of Di-I-labeled nerve fibers (arrows) in the ophthalmic nerve and the tracer-labeled neurons in the ophthalmic subdivision. (D) High-power magnification of TG neurons demonstrating the Di-I labeling, which fills the whole cell body homogeneously, whereas Di-I-negative neurons (arrows) exhibited only an unspecific fluorescence signal confined to lipofuscin granules (E). Scale bars: A and B, 5 mm; C, 300 μm; D and E, 50 μm.

sclera (5, 24), and lacrimal gland (1), resulted in retrogradely labeled neurons predominantly in the ophthalmic subdivision. Although there are reports suggesting an additional innervation of the orbit through the maxillary nerve (22), this is mostly attributed to variability between animals (17). Our findings based on postmortem Di-I tracing indicate that the human TG is somatopically organized in a fashion similar to that of monkeys with a modest degree of overlap between the trigeminal subdivisions.

Only four of the 12 TG assessed by LAT in situ hybridization showed single LAT-positive neurons in the ophthalmic division (V1). In contrast, the maxillary (V2) and mandibular (V3) divisions of all TG contained numerous LAT-positive neurons. Thus, the observed distribution of LAT mirrors the clinically observed frequency of herpes labialis and herpetic eye disease in humans: while the former is very frequent, the latter is a rare condition. However, once an episode of herpetic eye infection occurs, re-

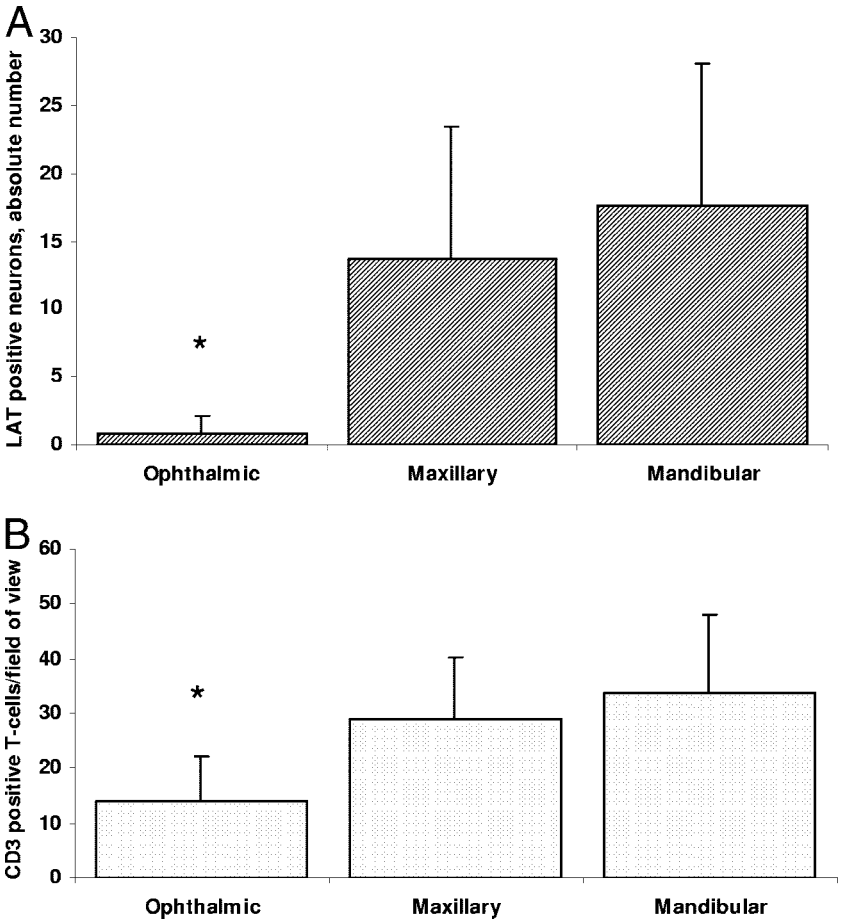

FIG. 3. Assessment of LAT-positive neurons and T cells in the three neural divisions of the TG. (A) The neurons projecting to the V2 and V3 branches of human TG contained significantly higher LAT signal (V2, 13.7 ± 9.7; V3, 17.6 ± 10.5) than those of the V1 branch (0.8 ± 1.4; Kruskal-Wallis ANOVA; $P < 0.0001$). (B) T cells clustered around the neurons in the V2 and V3 portions of the TG (V2, 29.1 ± 11.2/field of view; V3, 33.7 ± 14.3/field of view), while significantly fewer T cells surrounded the neurons in the V1 branch (14 ± 8.1; Kruskal-Wallis ANOVA; $P = 0.0007$).

lapses have a frequency similar to that of oral manifestations (13, 16), depending on the then-established HSV-1 latency in the neurons projecting to the V1. It is conceivable that the probability of reactivation is determined by the load of latent virus after a primary infection, regardless of whether it is symptomatic or asymptomatic. Studies using the HSV-1 animal model have indicated that the viral genome copy number has some impact on the HSV-1 reactivation frequencies (25).

In view of the present anatomical findings, the few HSV-1-infected neurons in V1 are possibly the result of the modest overlap between the maxillary and ophthalmic divisions seen in human TG. Alternatively, latent HSV-1 infection of V1 could occur after a primary infection or reactivation of HSV-1 in the mouth and cross-contamination of the ocular tissue. Thus far, it is still not clear whether a primary HSV-1 ocular infection has to occur in order to establish latency in the neurons of the V1 division. Lack of tissue damage or any residue from past tissue damage in human TG latently infected by HSV-1 (3, 29) does not support the theory that HSV-1 is transferred by local viral spread during reactivation within the ganglion itself.

Our group (29) and others (35) have shown that HSV-1 latency in human TG is accompanied by a chronic inflammation consisting mainly of $CD8^+$ T cells with a memory effector phenotype which are clonally expanded (3). This phenomenon was seen earlier in the HSV-1 mouse model (2, 15), and there is convincing evidence that T cells are implicated in blocking HSV-1 from reactivation (10, 14). In addition, it has been shown in the HSV-1 mouse model that only T cells that are HSV-1 specific express cytolytic granules (34). Once the viral antigen is cleared, cytotoxic $CD8^+$ T cells downregulate cytolytic molecule transcription (18). Recently it was demonstrated that the $CD8^+$ T-cell lytic granule component granzyme B can block the HSV-1 life cycle through a nonlytic mechanism (11). Granzyme B can directly cleave the viral protein ICP4, which is required for efficient transcription of early and late viral genes (11). In the present study, we compared the $CD8^+$ T-cell infiltration and the expression of cytolytic granules of granzyme B in the ophthalmic versus maxillary and mandibular divisions. $CD8^+$ T cells were found in all three divisions of the TG and also in the respective nerves; however, they were clearly abundant and occurred in clusters only in V2 and V3. A

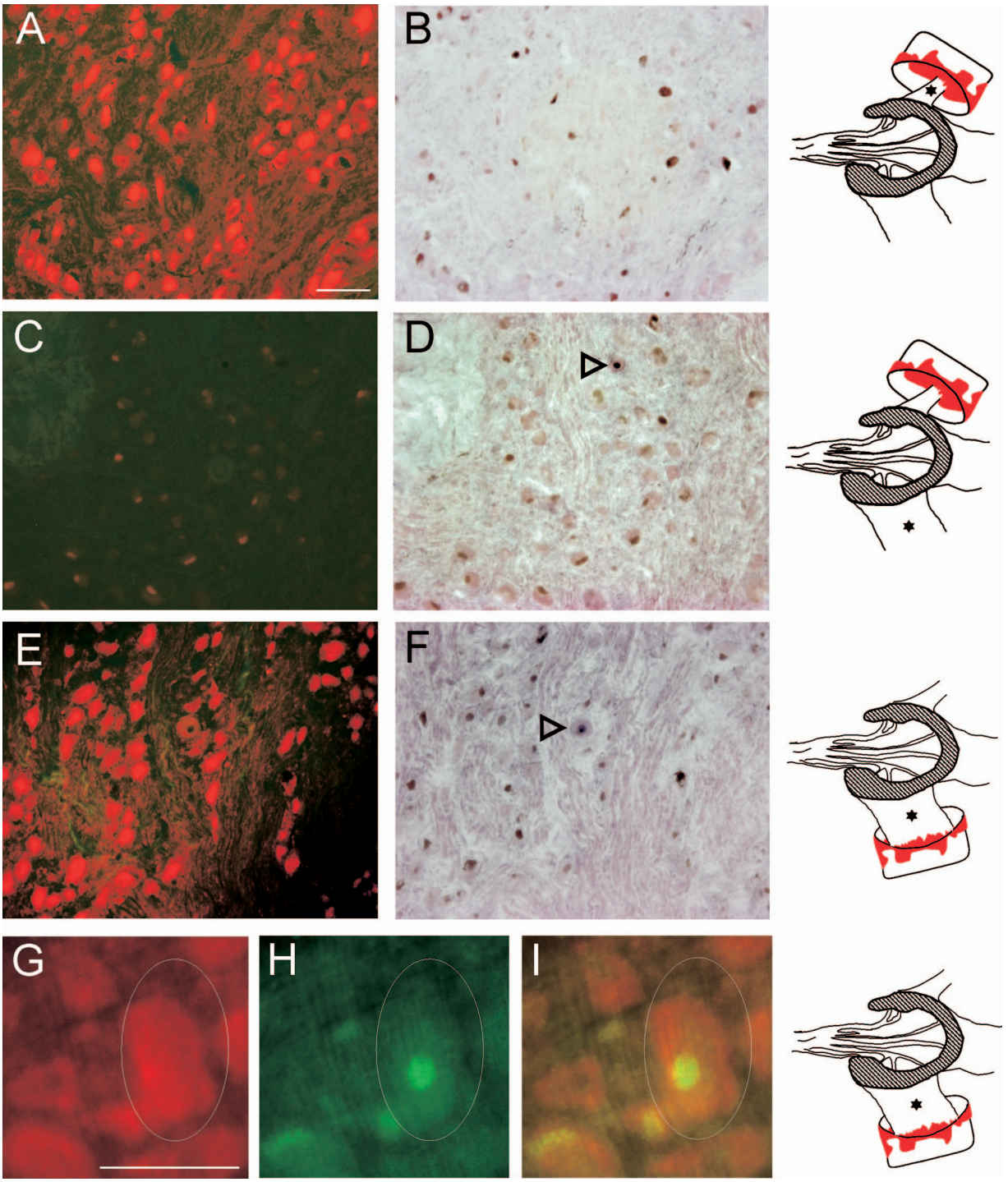

FIG. 4. Di-I tracing followed by LAT in situ hybridization in the three divisions of human TG. The pictures in the first column (A, C, and E) show the divisions after Di-I tracer, those in the second column (B, D, and F) depict LAT in situ hybridization of the same region, and a pictogram in the third column indicates which branch of the TG was traced with Di-I and which branch is shown in the photographs (indicated by an asterisk). No LAT signal was found in the traced ophthalmic branch (B). LAT was clearly visible in the untraced (D) and traced (F) mandibular branch (empty arrowhead). The bottom row (G to I) shows LAT FISH in the traced mandibular division. (G and H) Traced neuron (G) expressing LAT (hybridization to a fluorescein isothiocyanate-labeled oligonucleotide [H]). Panel I shows a merged picture (yellow nucleus). The scale bar (10 μm in all photographs) in panel A is also applicable to the micrographs in panels B to F; that in panel G is also applicable to the micrographs in panels H and I.

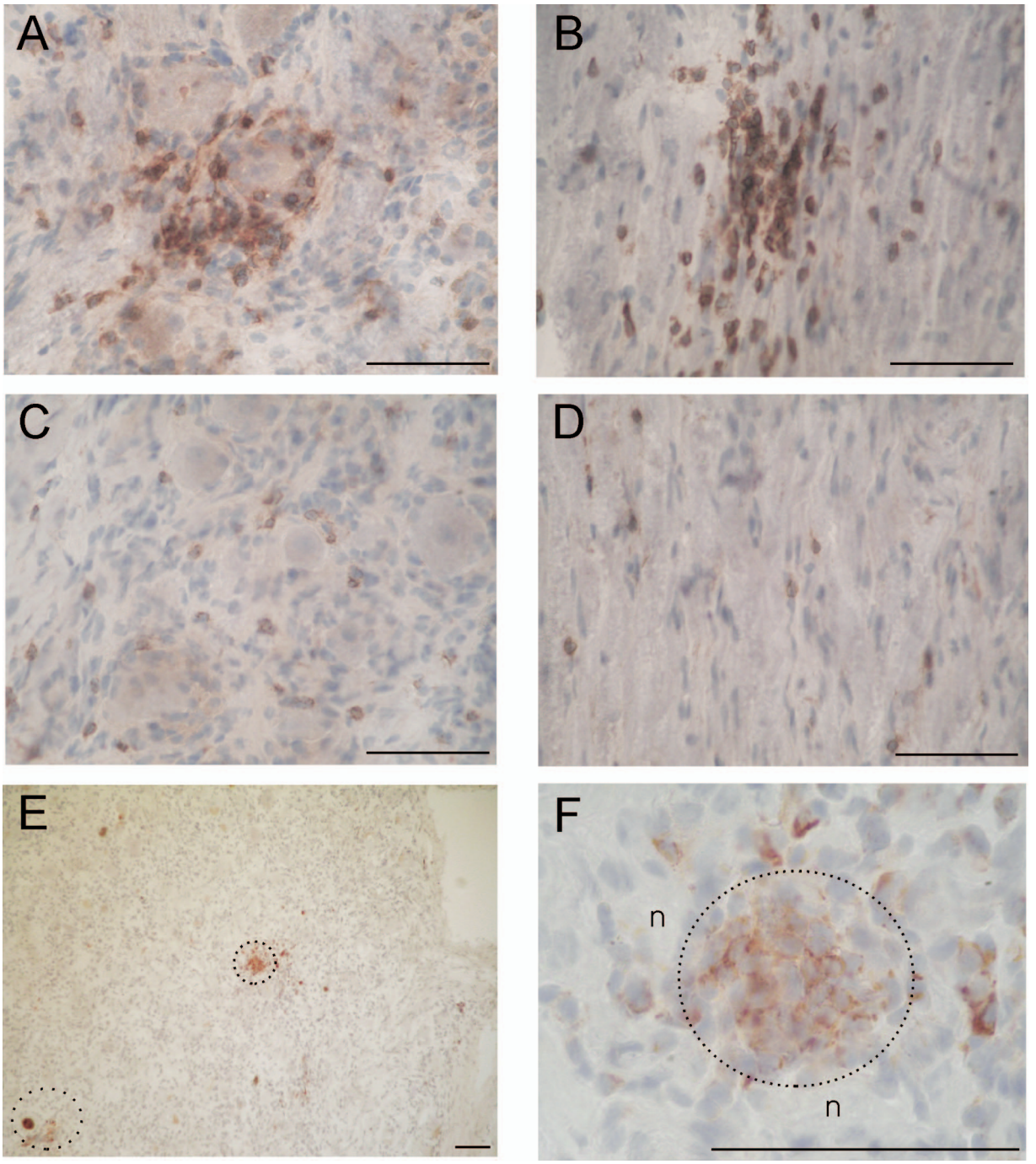

FIG. 5. Distribution of cytotoxic T cells in the ophthalmic and maxillary divisions and nerves of human TG. $CD8^+$ T cells are arranged around a sensory neuron (A) and clustered in nerve fibers (B) of the maxillary division (V2). Single $CD8^+$ T cells are scattered among sensory neurons (C) and nerve fibers (D) of the ophthalmic division (V1). Also shown are groups of granzyme B-positive T cells in V2 (E; two dotted circles). Panel F shows a higher magnification of the centered cluster (dotted circle; n, sensory neurons [×1,000]). The scale bars are 10 μm in all micrographs.

significant correlation between the presence of T cells and LAT in the neurons projecting to the three branches of the TG was found. This is in line with our previous study, where we demonstrated that LAT and T-cell clusters could only be found in the TG, while the dorsal root ganglia were LAT negative and contained only single, scattered T cells (7). Only a few T cells surrounding neurons in the V2 and V3 ganglionic divisions expressed granzyme B and occasionally occurred in clusters. This again stresses that viral activity goes on mainly in the V2 and V3 divisions.

In conclusion, the distribution of latent HSV-1 and cytotoxic T cells in the three divisions of the TG mirrors the frequency

of reactivation in the oral and eye regions and the mode of infection with HSV-1, which is influenced by human trigeminal anatomy.

ACKNOWLEDGMENTS

This study was supported by a DFG grant to D.T. and T.D. (TH 894/3-1), a DFG grant to A.H. (Ho 1639/4-3), and a grant from the Friedrich Baur-Foundation to K.H.

We thank Judy Benson for copyediting the manuscript.

REFERENCES

1. **Baljet, B., and F. VanderWerf.** 2005. Connections between the lacrimal gland and sensory trigeminal neurons: a WGA/HRP study in the cynomolgous monkey. J. Anat. **206:**257–263.
2. **Cantin, E. M., D. R. Hinton, J. Chen, and H. Openshaw.** 1995. Gamma interferon expression during acute and latent nervous system infection by herpes simplex virus type 1. J. Virol. **69:**4898–4905.
3. **Derfuss, T., S. Segerer, S. Herberger, I. Sinicina, K. Hüfner, K. Ebelt, H. G. Knaus, I. Steiner, E. Meinl, K. Dornmair, V. Arbusow, M. Strupp, T. Brandt, and D. Theil.** 2007. Presence of HSV-1 immediate early genes and clonally expanded T-cells with a memory effector phenotype in human trigeminal ganglia. Brain Pathol. **17:**389–398.
4. **Gallyas, F.** 1979. Silver staining of myelin by means of physical development. Neurol. Res. **1:**203–209.
5. **Gentle, A., and G. L. Ruskell.** 1997. Pathway of the primary afferent nerve fibres serving proprioception in monkey extraocular muscles. Ophthalmic Physiol. Opt. **17:**225–231.
6. **Hill, J. M., F. Sedarati, R. T. Javier, E. K. Wagner, and J. G. Stevens.** 1990. Herpes simplex virus latent phase transcription facilitates in vivo reactivation. Virology **174:**117–125.
7. **Hüfner, K., T. Derfuss, S. Herberger, K. Sunami, S. Russell, I. Sinicina, V. Arbusow, M. Strupp, T. Brandt, and D. Theil.** 2006. Latency of alpha-herpes viruses is accompanied by a chronic inflammation in human trigeminal ganglia but not in dorsal root ganglia. J. Neuropathol. Exp. Neurol. **65:**1022–1030.
8. **Kaye, S., and A. Choudhary.** 2006. Herpes simplex keratitis. Prog. Retin. Eye Res. **25:**355–380.
9. **Kaye, S. B., C. Lynas, A. Patterson, J. M. Risk, K. McCarthy, and C. A. Hart.** 1991. Evidence for herpes simplex viral latency in the human cornea. Br. J. Ophthalmol. **75:**195–200.
10. **Khanna, K. M., R. H. Bonneau, P. R. Kinchington, and R. L. Hendricks.** 2003. Herpes simplex virus-specific memory CD8+ T cells are selectively activated and retained in latently infected sensory ganglia. Immunity **18:**593–603.
11. **Knickelbein, J. E., K. M. Khanna, M. B. Yee, C. J. Baty, P. R. Kinchington, and R. L. Hendricks.** 2008. Noncytotoxic lytic granule-mediated CD8+ T cell inhibition of HSV-1 reactivation from neuronal latency. Science **322:**268–271.
12. **Labetoulle, M., S. Maillet, S. Efstathiou, S. Dezelee, E. Frau, and F. Lafay.** 2003. HSV1 latency sites after inoculation in the lip: assessment of their localization and connections to the eye. Investig. Ophthalmol. Vis. Sci. **44:**217–225.
13. **Liesegang, T. J.** 2001. Herpes simplex virus epidemiology and ocular importance. Cornea **20:**1–13.
14. **Liu, T., K. M. Khanna, X. Chen, D. J. Fink, and R. L. Hendricks.** 2000. CD8(+) T cells can block herpes simplex virus type 1 (HSV-1) reactivation from latency in sensory neurons. J. Exp. Med. **191:**1459–1466.
15. **Liu, T., Q. Tang, and R. L. Hendricks.** 1996. Inflammatory infiltration of the trigeminal ganglion after herpes simplex virus type 1 corneal infection. J. Virol. **70:**264–271.
16. **Lorette, G., A. Crochard, V. Mimaud, P. Wolkenstein, J. F. Stalder, and A. El Hasnaoui.** 2006. A survey on the prevalence of orofacial herpes in France: the INSTANT Study. J. Am. Acad. Dermatol. **55:**225–232.
17. **Marfurt, C. F., and S. F. Echtenkamp.** 1988. Central projections and trigeminal ganglion location of corneal afferent neurons in the monkey, Macaca fascicularis. J. Comp. Neurol. **272:**370–382.
18. **Mintern, J. D., C. Guillonneau, F. R. Carbone, P. C. Doherty, and S. J. Turner.** 2007. Cutting edge: tissue-resident memory CTL down-regulate cytolytic molecule expression following virus clearance. J. Immunol. **179:**7220–7224.
19. **Perng, G. C., C. Jones, J. Ciacci-Zanella, M. Stone, G. Henderson, A. Yukht, S. M. Slanina, F. M. Hofman, H. Ghiasi, A. B. Nesburn, and S. L. Wechsler.** 2000. Virus-induced neuronal apoptosis blocked by the herpes simplex virus latency-associated transcript. Science **287:**1500–1503.
20. **Polcicova, K., P. S. Biswas, K. Banerjee, T. W. Wisner, B. T. Rouse, and D. C. Johnson.** 2005. Herpes keratitis in the absence of anterograde transport of virus from sensory ganglia to the cornea. Proc. Natl. Acad. Sci. USA **102:**11462–11467.
21. **Porter, J. D., B. L. Guthrie, and D. L. Sparks.** 1983. Innervation of monkey extraocular muscles: localization of sensory and motor neurons by retrograde transport of horseradish peroxidase. J. Comp. Neurol. **218:**208–219.
22. **Ruskell, G. L.** 1974. Ocular fibres of the maxillary nerve in monkeys. J. Anat. **118:**195–203.
23. **Ruskell, G. L.** 1985. Innervation of the conjunctiva. Trans. Ophthalmol. Soc. U. K. **104:**390–395.
24. **Ruskell, G. L.** 1994. Trigeminal innervation of the scleral spur in cynomolgus monkeys. J. Anat. **184:**511–518.
25. **Sawtell, N. M., D. K. Poon, C. S. Tansky, and R. L. Thompson.** 1998. The latent herpes simplex virus type 1 genome copy number in individual neurons is virus strain specific and correlates with reactivation. J. Virol. **72:**5343–5350.
26. **Shuster, J. J., H. E. Kaufman, and A. B. Nesburn.** 1981. Statistical analysis of the rate of recurrence of herpesvirus ocular epithelial disease. Am. J. Ophthalmol. **91:**328–331.
27. **Sparks, D. L., L. F. Lue, T. A. Martin, and J. Rogers.** 2000. Neural tract tracing using Di-I: a review and a new method to make fast Di-I faster in human brain. J. Neurosci. Methods **103:**3–10.
28. **Stevens, J. G., E. K. Wagner, G. B. vi-Rao, M. L. Cook, and L. T. Feldman.** 1987. RNA complementary to a herpesvirus alpha gene mRNA is prominent in latently infected neurons. Science **235:**1056–1059.
29. **Theil, D., T. Derfuss, I. Paripovic, S. Herberger, E. Meinl, O. Schueler, M. Strupp, V. Arbusow, and T. Brandt.** 2003. Latent herpesvirus infection in human trigeminal ganglia causes chronic immune response. Am. J. Pathol. **163:**2179–2184.
30. **Theil, D., I. Paripovic, T. Derfuss, S. Herberger, M. Strupp, V. Arbusow, and T. Brandt.** 2003. Dually infected (HSV-1/VZV) single neurons in human trigeminal ganglia. Ann. Neurol. **54:**678–682.
31. **Thompson, R. L., and N. M. Sawtell.** 1997. The herpes simplex virus type 1 latency-associated transcript gene regulates the establishment of latency. J. Virol. **71:**5432–5440.
32. **Tullo, A. B., D. L. Easty, T. J. Hill, and W. A. Blyth.** 1982. Ocular herpes simplex and the establishment of latent infection. Trans. Ophthalmol. Soc. U. K. **102:**15–18.
33. **VanderWerf, F., C. Buisseret-Delmas, and P. Buisseret.** 2002. Afferent innervation of eyelids and their connections to the superior colliculus. Mov. Disord. **17:**8–11.
34. **van Lint, A. L., L. Kleinert, S. R. M. Clarke, A. Stock, W. R. Heath, and F. R. Carbone.** 2005. Latent infection with herpes simplex virus is associated with ongoing $CD8^+$ T-cell stimulation by parenchymal cells within sensory ganglia. J. Virol. **79:**14843–14851.
35. **Verjans, G. M., R. Q. Hintzen, J. M. van Dun, A. Poot, J. C. Milikan, J. D. Laman, A. W. Langerak, P. R. Kinchington, and A. D. Osterhaus.** 2007. Selective retention of herpes simplex virus-specific T cells in latently infected human trigeminal ganglia. Proc. Natl. Acad. Sci. USA **104:**3496–3501.